Characterizing observed environmental variability with HF Doppler radar surface current mappers and Acoustic Doppler current profilers.

Josh T. Kohut
Coastal Ocean Observation Lab
Rutgers University

Hugh J. Roarty
Coastal Ocean Observation Lab
Rutgers University

Scott M. Glenn
Coastal Ocean Observation Lab
Rutgers University

Abstract- A network of High Frequency (HF) radars are deployed along the New Jersey coast providing synoptic current maps across the entire shelf. These data serve a variety of user groups from scientific research to Coast Guard search and rescue. In addition, model forecasts have been shown to improve with surface current assimilation. In all applications, there is a need for better definitions and assessment of the measurement uncertainty. During a summer coastal predictive skill experiment in 2001, an array of in situ current profilers were deployed in the vicinity of two HF radar sites, one long range and one standard range system. Comparisons statistics were calculated between different vertical bins on the same current profiler, between different current profilers, and between the current profilers and the different HF radars. The vertical and horizontal shears were then characterized using the observed RMS differences. We further focused on two cases, one with relatively high vertical shear, and a second with relatively low vertical shear. Observed differences between the top bin of the current profiler and the HF radar were influenced by both system accuracy and the environment. Using the in situ current profilers, the environmental variability over scales based on the HF radar sampling was quantified. HF radar comparisons with the current profilers were on the same order as the observed environmental shears, indicating that the environment has a significant influence on the observed differences. Both vertical and horizontal shears contribute to these differences. When the potential effects of the vertical shear could be minimized, the remaining difference between the current profiler and the HF radar was similar to the horizontal shear (~2.5 cm/s) and below the digitization interval of the raw radial data at the time of the deployment.

I. Introduction

Coastal ocean current mapping using High Frequency (HF) radar has matured to the point where it is now considered an essential component of regional ocean observing systems. HF Radar networks are being constructed with high-resolution standard-range systems nested within lower resolution, long-range systems. HF radar also provides a relatively new but important spatial dataset for assimilation into coastal forecast models, enabling us to advect and evolve features into the future. Several data assimilation studies [1], [2], [3] have recently tested new methods to assimilate CODAR HF radar data. Wilkin et al. [3] have shown that CODAR HF radar surface current maps combined with subsurface CTD data assimilated via intermittent melding produce the greatest improvements in model forecasts when compared to withheld validation data. These data assimilation studies require the specification of uncertainties. HF radar uncertainties are set at two levels, first at the level of the radial currents from individual radars, second at the level of the total vector currents constructed from multiple radars.

HF radar surface currents have been validated at both levels with many different types of in situ current measurements, including surface drifters and subsurface current meters. To date, much of the validation has focused on the higher resolution HF radar systems. These analyses cite differences between HF radar measurements and various in situ measurements on the order of 9 to 27 cm/s (for a review see [4]). In all of these studies, the instruments used for "ground truth" measure the currents over different spatial and/or temporal scales than those of the HF radar site being validated.

Since HF radar uses the scattered signal off surface gravity waves to measure the ocean current, the observations are limited to the ocean surface. Even with modern

subsurface acoustic current profilers, the depth of the measurement bin closest to the surface differs from the surface radar measurement by a few meters. Any vertical shear in the upper water column will contribute to differences between the two measurements. A drifter, while at the surface, is a Lagrangian measurement and spends only a finite amount of time within each HF radar cell. Spatially, an HF radar measurement cell can be as large as 3 km^2 for a standard range system compared to a point measurement of a sub-surface current meter. For a long-range system, this area can be as large as 20 km^2. Any horizontal shear over scales of the radar cell will contribute to observed differences. In the past, validation studies acknowledged that these discrepancies exist but do not go on to quantify the real environmental shear during the validation analysis [5]. Without knowing the magnitude of the horizontal and vertical shear over the relevant scales during the study period, there is no way to conclude what part of the observed difference is due to system uncertainties and what part is due to real environmental shears.

In this analysis an array of Acoustic Doppler Current Profilers (ADCPs) are used to quantify the vertical and horizontal shears over the same scales as the HF radar cells. Comparisons are then drawn between various ADCP bins and the closest long-range HF radar measurement cell. The observed differences between the HF radar and in situ current measurements are then put into the context of the observed shears. The combined CODAR/ADCP data were then used to characterize the shear in the upper water column during two events, one with high vertical shear and one with low vertical shear.

II. Background

Rutgers University operates a nested array of CODAR-type HF radar systems. CODAR is a direction finding system that uses a compact receive antenna design with three elements, two directionally dependent loops and a single omni-directional monopole [6], [7], [8]. With an operating frequency around 5 MHz, the long-range CODAR systems measure surface currents within the upper 1.6 meters of the water column [9]. Typical spatial resolutions are on the order of 6 km in range and 5 degrees in azimuth with maximum ranges exceeding 200 km. Four long-range sites along the coast of New Jersey from Wildwood to Sandy Hook provide surface current maps over the entire New Jersey Shelf (Fig. 1). These four sites form one cluster of systems within the NorthEast Observing System (NEOS).

Nested within the long-range system are two standard range sites originally deployed along the southern New Jersey coast [10], [11] and recently moved to the New York Bight Apex to support river plume research (Fig. 1). With an operating frequency of 25 MHz, these systems measure the current within the upper 30 cm of the water column [9]. Typical spatial resolutions are on the order of 1 km in range and 5 degrees in azimuth with maximum ranges out to 40 km.

III. Methods

A. HF radar setup

The comparisons presented here will focus on a single standard-range system deployed in Brigantine, NJ and a single long-range system deployed in Tuckerton, NJ

(Fig. 1). These particular sites were chosen because they provide overlapping coverage of the region occupied by the ADCPs (Fig. 2) and sample over different space and time scales (Table I). In addition, this analysis will concentrate on the first level of error bars, the radial level. Since the total vector error bars are based on the radial uncertainties with the geometric errors introduced in the vector combination [12], understanding the accuracy of the radial vectors is crucial when quantifying HF radar uncertainty.

The long-range site operates at 4.55 MHz with a sweep width of 25 KHz, giving an average range of 180 km and a range resolution of 5.85 km. Raw cross-spectra were created every 17 minutes using a 1024-point FFT. These spectra were then hourly averaged, centered on each half hour (Table I). Using the MUltiple SIgnal Classification (MUSIC) direction finding algorithm [13], [14] with the measured beam patterns [10], [15], these overlapping hourly averaged spectra were used to generate radial current maps. These radial current vector maps were then averaged into four-hour files generated every three hours. Any given gridpoint in the field could have up to seven vectors going into the final average. For example, a file at 12:00 GMT was generated with hourly averaged radial files centered at 10:30, 11:00, 11:30, 12:00, 12:30, 13:00, and 13:30.

The standard site operated at 24.7 MHz with a sweep width of 100 KHz giving an average range of 40 km and a range resolution of 1.51 km (Table I). The raw cross spectra were written every 4.27 minutes using a 512-point FFT and used to create 15-minute radial files, outputted every ten minutes. These 10-minute files were then averaged into hourly files.

The two different sampling schemes of the long and standard range systems are due to the differences in the transmitted signal. Since CODAR is a Doppler radar, the

currents are frequency offsets, converted into radial velocity components. The frequency resolution of the spectra is dependent on the operating frequency, sweep rate, and FFT length used in the processing. The long-range system, with a 1 Hz sweep rate and an operating frequency of 4.55 MHz, needs a 1024 point FFT length to resolve currents to 3.22 cm/s. The standard system, with a sweep rate of 2 Hz and an operating frequency of 24.7 MHz, needs a 512 point FFT to resolve currents to 2.31 cm/s.

B. ADCP Setup

Two bottom mounted RD Instruments ADCPs were deployed off the coast of New Jersey near the Longterm Ecosystem Observatory (LEO) as part of the Coastal Predictive Skill Experiments (CPSE) [16], [17] (Fig. 2). They were deployed for 37 days between July 10, 2001 and August 16, 2001. The inshore ADCP at COOL3 was moored in 18 meters of water. The second ADCP at COOL5, 8 km further offshore, was moored in 22 meters of water. In addition to the current profile data, there was a string of thermisters running the entire water column at each ADCP, sampling every ten minutes through the study period. The ADCPs operated at 600 KHz with a bin resolution of one meter. Each continuously sampled with 5 second ensembles in mode-1. Sidelobe contamination limits the ability of ADCPs to measure the currents up to the surface. For typical Janus configuration, this is usually 10% of the water depth, which in this case is 1.8 m and 2.2 m. Thus a bin centered at 2.5 meters below the surface is expected to be contaminated, and a 1 m bin centered at 3.5 m below the surface is expected to be good. This was checked against the percent good data return calculated with the RD software package. For both ADCPs the bin 3.5 m below the surface had over 98% good data

return. The ADCP data was averaged to exactly match the CODAR processing. For the long-range site comparisons, the ADCP was first averaged into hourly files generated every half hour, and then these hourly files were averaged into four-hour files generated every three hours. For the standard site comparison, the ADCP data was first averaged into 15-minute files generated every 10 minutes. These 10-minute files were then averaged into 1.25 hourly files generated every hour. Both datasets were rotated into a radial and cross-radial coordinate system to match the CODAR data. Both the CODAR and ADCP data were detided using a least squared fit of the dominant constituent, M_2, to the raw data. Only concurrent ADCP and CODAR data were used in the least squares fit.

Since the COOL5 ADCP is not centered directly in any of the long-range radar cells (Fig. 2), the radial data was spatially interpolated to the ADCP. The CODAR processing treats each range bin separately. For each range bin, spectra are run through the MUSIC algorithm to calculate the bearing of each radial velocity within the first order Bragg region. The number of radial vectors in any given range cell depends on (i) the digitization interval determined by the FFT length, operating frequency, and sweep rate and (ii) the number of antenna elements in the receive array. The digitization interval controls how many radial velocity vectors are available, and the number of antenna elements determines the number of possible MUSIC solutions for each radial velocity. For our setup with three receive antenna elements, a radial velocity every 3.22 cm/s (2.31 cm/s) for the long-range (standard range) system can be placed in up to two angular bins. Consequently if there are more than two angles with a given radial velocity or periods of weak surface currents, data coverage will be reduced. Based on these constraints, the interpolation was done in angle, not range. This is consistent with previous interpolation

techniques used on the standard-range dataset [10], [18]. Using the four bins surrounding the ADCP, two on either side, the radial data were averaged with weights chosen based on the distance of each bin from the ADCP. The center of the two closest bins is three times closer to the ADCP than the center of the two outermost bins, so the two bins adjacent to the ADCP were weighted three times the two bins further away (Fig. 3). The angular swath and weighting of the interpolation is consistent with the 20-degree half-beam width of an ideal 300m linear phased array operating at 5 MHz. For each four-hour file, a value was calculated only if at least two of the four angular CODAR bins contained data. Comparisons of the ADCP were produced with both the non-interpolated and interpolated data. Since most of the previous validation studies have focused on the standard range systems and the orientation of the long-range bins better match the ADCP locations (Fig 2.), the majority of the analysis focuses on the long-range data.

IV. Contribution of Time Sampling and Environmental Shears

A. Time averaging

Doppler processing identifies a number of radial current velocities observed in the Bragg peaks of the N antennas in the compact array. A direction finding algorithm then places each of the observed radial velocities in at most N-1 directions. The effect of varying data coverage is seen when the hourly files (generated every half hour) are averaged over four hours. If the data were complete, 7 vectors would go into the average for each of the gridpoints in the field. Reduced data coverage will lead to less hourly vectors used in the final average. To simulate this, the continuous ADCP record was

compared to the same ADCP data with random hourly vectors missing in the four-hour averages. Different time series were constructed with different minimum requirements of vectors going into the four-hour average. The minimum number ranged from 1 to 7 vectors, where 7 vectors would be a complete record. This was done for two cases. One compared the complete record of the top ADCP bin at COOL5 to the incomplete records at the same location. The second compared the complete record of the top ADCP bin at COOL3 with incomplete records at that same location. For case one, as the number of hourly data used in the average increases, the RMS difference between the complete and incomplete dataset decreases (Table II). If the minimum requirement is set to one, the RMS difference was 4.27 cm/s. When the minimum requirement was increased to 2 vectors, the RMS difference reduced to 2.82 cm/s. Increasing the minimum requirement from 1 vector to 2 decreased the RMS difference by almost half. Above 2, the RMS difference slowly decreased with larger minimum requirements, eventually reaching 0. For case two, the RMS difference dropped from 3.63 cm/s with one vector to 2.25 cm/s with 2 vectors. As the number of vectors increased from 2 to 7, the RMS difference gradually decreases to 0 cm/s. For both cases the largest improvement occurred when the minimum requirement was increased from one vector to two vectors. In addition the requirement of two or more vectors going into the average lowers the RMS difference to the current resolution of the standard range site and below the current resolution of the long-range site Based on these data, the CODAR data were further sorted to have at least two hourly vectors in each four hour average to be included in the validation.

B. Observed environmental shears

Using the two ADCPs, the horizontal and vertical variability during the study period was quantified. The variability was measured across the scales relevant to the comparison. In the vertical, the long-range and standard-range CODAR are measuring the velocity within the upper 1.5 to 0.3m of the water column while the closest ADCP bin is 3.5 m below the surface. In the horizontal, the ADCP is sampling at a point while the standard and long-range sites were sampling across a length scale of 1.5km and 6 km, respectfully.

In the vertical, the top ADCP bin at COOL5, 3.5 m below the surface, was compared to another bin of the same ADCP, 6.5 m below the surface (Fig. 4a). The RMS difference between these two bins over the study period was 6.25 cm/s for the raw currents and 0.63 cm/s for the M_2 tide (Table III). These two bins were chosen because the vertical separation was on the same order as that between the surface CODAR measurement and the top bin of the ADCP. Since the tides in this region vary much less over the depth and spatial scales discussed here, the vertical shear is much less than that seen in the raw currents.

In the horizontal, the surface bin at COOL5 was compared to the surface bin of COOL3, 8 km away. 8 km is similar to the horizontal length scale of the long-range measurement. During this particular study period, the observed RMS difference was 5.22 cm/s for the raw data and 1.22 cm/s for the tidal data (Table III). Once again the difference in the tides was much less than that seen in the raw currents. Over the study period, both the horizontal and vertical shear was on the order of 5-6 cm/s for the raw velocity fields, and 1.0 cm/s for the tidal fields.

The estimated contribution of the environmental shears to the observed differences between the long-range CODAR site and the top bin of the ADCP were on the order of 5 cm/s. Additionally, data dropouts could contribute differences on the same order intermittently through the study period. Comparisons between the ADCPs and the long-range and standard-range CODAR sites were analyzed in the context of the scale of these contributions.

V. HF Radar/ADCP comparisons

A. Vertical difference

Radial current time series of the COOL5 ADCP bin closest to the surface was compared to the radial data of the CODAR range and angular bin closest to the ADCP (Fig. 4b). The RMS difference over the study period for the raw radial velocity was 5.86 cm/s and reduced to 4.32 cm/s for the long-range CODAR data interpolated to the ADCP location (Table III). This difference was of the same order as the vertical shear measured with the ADCP alone. The tidal velocity comparison significantly improved with an RMS difference of 0.71 cm/s and 0.18 cm/s for the closest bin and interpolated data, respectfully. These differences were consistent with the observed vertical shear in the tidal velocity at COOL5.

B. Horizontal difference

The RMS difference between the CODAR bin closest to the ADCP at COOL5 and the top bin of the ADCP at COOL3 was 6.3 cm/s for the raw velocity and 2.22 cm/s for the tidal velocity (Table III). The horizontal shear measured between COOL3 and

COOL5 was 5.22 cm/s for the raw velocity and 1.22 cm/s for the tidal velocity. Once again this difference was on the same order as the RMS difference due to the shear measured between the two ADCPs.

The RMS difference was also calculated between the ADCP and the standard range system. Recall that the standard system sampled across a smaller spatial area and closer to the ocean surface than the long-range system. Therefore the standard site velocity was further (closer to the surface) from the top bin of the ADCP than the deeper long-range measurement and closer in spatial scale to the ADCP than the larger long-range cell (Fig. 2). When we compare the standard system to the ADCP, the raw velocity RMS difference was 6.4 cm/s. This was on the same order as the long-range comparison but slightly larger. The larger difference could be due to the shallower measurement, further from the top bin of the ADCP. When looking at the standard-range, long-range, and spatially separated ADCPs, the significance of the horizontal and vertical shear was clear. Both the horizontal and vertical shear must be considered when comparing HF radar data to in situ current measurements.

For both the vertical and horizontal direction the observed differences between the ADCPs and CODAR were of the same order as the differences observed between the two ADCPs over the same scales. When the environmental variability is as large as the difference between two different current measurements with observations sampling over the same scales, it is difficult to determine exactly what is due to the local environment. These results suggest that the difference observed between the ADCP and CODAR were more representative of the environment, rather than the accuracy of either instrument.

Since the environmental variability had significant influence on the observed shear, we used the RMS difference as a tool to characterize the shear in the upper water column. To analyze the influence of each component of shear separately, the ADCPs were used to identify two specific events, one with high vertical shear and one with low vertical shear relative to the measured horizontal shear.

VI. The influence of shear

During the study period there were events in which the vertical shear exceeded the observed horizontal shear, and events in which the horizontal shear exceeded the vertical shear. Within a subset of the data between yd 209 and yd 214 (July 28, 2001 to August 2, 2001), both cases occur within a few days of each other. Yd 209 and 210 are characterized by a relatively strong thermocline and weak upwelling winds (Fig. 5). The winds change to a downwelling favorable direction on yd 211, deepening the thermocline and weakening the stratification. After this mixing event the wind returns to the upwelling favorable direction and the weaker thermocline shallows. The downwelling event mixes the water column and reduces the strength of the stratification.

A. Low vertical shear event (vertical component < horizontal component)

Between yd 209 and yd 211 the RMS difference between the 3.5 m and 6.5 m bin of the ADCP at COOL5 was 2.22 cm/s. During this two-day period a very strong thermocline separated the surface layer from the effects of bottom friction, resulting in a 10 m deep surface layer with very low vertical shear (Fig. 5a). The temperature profile at COOL5 averaged over these two days showed a surface layer at 22°C that extends down

to 10 m (Fig. 5a). Below this layer the temperature quickly changes to 14°C. The RMS difference between the interpolated CODAR and the top bin at COOL5 is 3.80 cm/s. This comparison was extended throughout the water column with each bin of the ADCP. The RMS profile in the surface layer was relatively constant, around 2.80 cm/s with a minimum of 2.50 cm/s at 4.5 meters (Fig. 5a). There was a strong correlation between the location of the thermocline and the depth at which the ADCP velocity begins to differ significantly from the CODAR measurement. The peak in the RMS difference fell right in the middle of the thermocline. The vertical line in Figure 5a is the RMS difference between the top bins at COOL5 and COOL3 over this two-day subset and indicates an estimate of the magnitude of the RMS difference due to horizontal shear of 2.82 cm/s. This value was nearly the same as the RMS difference between CODAR and the entire surface layer measured by the ADCP. For this low vertical shear case, observed RMS differences in the upper water column indicate a relatively constant shear with a near zero vertical contribution and a horizontal contribution on the order of 3 cm/s.

B. High vertical shear example (vertical component > horizontal component)

Following the downwelling event, the RMS difference between the top (3.5 m) bin and the 6.5 m bin of the ADCP at COOL5 increased from 2.22 cm/s to 6.86 cm/s while the horizontal shear remained fairly steady, increasing from 2.82 cm/s to 2.88 cm/s. Even though there is still a thermocline separating the surface layer from the effects of bottom friction, the profile of the RMS difference looked significantly different (Fig. 5b). No longer was the RMS constant through the surface layer with a peak at the thermocline. In this higher vertical shear period the RMS difference increased linearly

throughout the surface layer and remained relatively constant through the bottom layer (Fig. 5b). The CODAR comparison starts at 3.98 cm/s at the top bin (3.5 m) and increases to 12.79 cm/s at the thermocline 10 meters down. In the high vertical shear event, the vertical component of the shear dominates the observed difference. The linear dependence of the difference with depth indicates that the magnitude of the vertical shear in the upper water column was relatively constant. Assuming this and extrapolating the trend upward, the 2.5 m ADCP bin, if uncontaminated by sidelobes, would likely have reached the point where the CODAR/ADCP RMS difference was similar to the horizontal COOL5/COOL3 ADCP RMS difference.

In both the high and low shear example, the environment significantly influenced the RMS difference. In the low shear case, the horizontal component dominated the RMS difference as indicated by a constant magnitude in the upper water column equal the horizontal shear. When the vertical component of the shear increased to almost double that of the horizontal, the profile of the RMS difference became depth dependent in the surface layer, increasing linearly to the thermocline. Here the shear in the upper water column was again relatively constant from the thermocline to the surface, but now the vertical component had the larger influence on the RMS difference.

VII. Summary and Conclusions

HF radar surface current maps are an important component of regional observing systems. As these systems become more prevalent and utilized, it is necessary to quantify and lower uncertainties at both the radial and total vector level. When time averaging of the ADCP was precisely matched to the time averaging interval of the CODAR, RMS differences between the CODAR radial velocity and the nearest ADCP

top bin were comparable to the ADCP to ADCP RMS difference due to either vertical or horizontal shear. When the vertical shear was reduced, the minimum CODAR/ADCP RMS difference was 2.5 cm/s, less than the ADCP/ADCP RMS difference of 2.82 cm/s. In this case, the real environment contributed more to the observed difference rather than observational uncertainties of either the ADCP or CODAR.

Since the environment dominated the RMS difference, it can be used as a tool to characterize the magnitude of the shear in the upper water column. For the two cases examined here, when the vertical shear was less than the horizontal shear (case 1), the magnitude of the total shear was constant through the surface layer, on the order of the measured horizontal shear. When the vertical shear was larger than the horizontal (case 2), the total shear was once again constant in the surface layer, dominated by the vertical component. In both events, the magnitude of the shear remains relatively steady from the surface to the thermocline. As the range cell size increases with the long-range systems, the instances where the vertical and horizontal components of the shear are comparable increases. For these systems both vertical and horizontal shears must be considered when quantifying the uncertainties of the observations.

The next step in lowering the HF radar uncertainties is to develop new methodologies to fill in the data gaps at the radial level. The present operational processing procedure is only one of the vast number of processing routes that can lead to total vector fields. With RMS differences between CODAR and ADCP on the order of a few cm/s, consistent with the observed shear, another step is longer FFT lengths to produce finer current digitization. We have already demonstrated that interpolation in direction consistent with the typical 20-degree half-beam width of a linear phased array

system both fills in coverage and improves comparisons with ADCP data. A systematic comparison of interpolation possibilities in range, bearing and time is required to fully resolve this issue.

References

[1] Oke, P.R., J.S. Allen, R.N. Miller, G.D. Egbert, and P.M. Kosro. 2002. Assimilation of surface velocity data into a primitive equation coastal ocean model. *Journal of Geophysical Research*, Vol. 107, No. C9, 3122, doi: 10.1029/2000JC000511.

[2] Paduan, J.D., and I. Shulman. 2004. HF Radar data assimilation in the Monterey Bay area. Journal of Geophysical Research, Vol. 109, C07S09, doi:10.1029/2003JC001949.

[3] Wilkin, J.L., H.G. Arango, D.B. Haidvogel, C.S. Lichtenwalner, S.M. Glenn, and K.S. Hedstrom. 2004. A Regional Ocean Modeling System for the Long-term Ecosystem Observatory. Journal of Geophysical Research, submitted.

[4] Chapman, R.D. and H.C. Graber, 1997: Validation of hf radar measurements. *Oceanography*, 10, 76-79.

[5] Graber, H.C., B.K. Haus, L.K. Shay and R.D. Chapman, 1997: Hf radar comparisons with moored estimates of current speed and direction: expected differences and implications. *J. Geophys. Res*, 102, 18,749-18,766.

[6] Barrick, D.E., M.W. Evens and B.L. Weber, 1977: Ocean surface currents mapped by radar. *Science*, 198, 138-144.

[7] Lipa, B.J. and D.E. Barrick. 1983: Least-squares methods for the extraction of surface currents from CODAR cross-loop data: application at ARSLOE. *IEEE J. Ocean. Engr*, OE-8, 226-253.

[8] Lipa, B.J. and D.E. Barrick, 1986: Extraction of sea state from hf-radar sea echo: mathematical theory and modeling. *Radio Sci*, 21, 81-100.

[9] Stewart, R.H. and J.W. Joy, 1974: Hf radio measurement of surface currents. *Deep-Sea Res.*, 21, 1039-1049.

[10] Kohut, J. T. and S. M. Glenn, 2003. Calibration of HF radar surface current measurements using measured antenna beam patterns. *J. Atmos. Ocean. Tech*., 1303-1316.

[11] Kohut, J. T., Glenn, S. M., Chant, R. J. 2004. Seasonal current variability on the New Jersey inner shelf. *Journal of Geophysical Research*. 109, C07S07, DOI: 10.1029/2003JC001963.

[12] Chapman, R.D., L.K. Shay, H.C. Graber, J.B. Edson, A. Karachintsev, C.L. Trump and D.B. Ross, 1997: On the accuracy of hf radar surface current measurements: intercomparisons with ship-based sensors. *J. Geophys. Res*, 102, 18,737-18,748.

[13] Barrick, D.E. and B.J. Lipa, 1999: Radar angle determination with MUSIC direction finding. United States Patent, No. 5,990,834.

[14] Schmidt, R.O., 1986: Multiple emitter location and signal parameter estimation. *IEEE Trans. Antennas Propag*, AP-34, 276-280.

[15] Barrick, D.E. and B.J. Lipa, 1986: Correcting for distorted antenna patterns in CODAR ocean surface measurements. *IEEE J. Ocean. Eng*, OE-11, 304-309.

[16] Chant, R. J., S. Glenn, J. Kohut, 2004: Flow reversals during upwelling conditions on the New Jersey inner shelf *J. Geophys. Res*., Vol. 109, No. C12, C12S03. 10.1029/2003JC001941

[17] Glenn, S. M., Arnone, R., Bergmann, T., Bissett, W. P., Crowley, M., Cullen, J., Gryzmski, J., Haidvogel. D., Kohut, J., Moline, M. A., Oliver, M., Orrico, C., Sherrell, R., Song, T., Weidemann, A., Chant, R., Schofield, O. 2004. The Biogeochemical impact of summertime coastal upwelling in the Mid-Atlantic Bight. Journal of Geophysical Research 109 C12S02, DOI:10.1029/2003JC002265.

[18] Paduan, J.D., D.E. Barrick, D.M. Fernandez, Z. Hallok and C.C. Teague, 2001: Improving the accuracy of coastal hf radar current mapping. *Hydro International*, 5, 26-29.

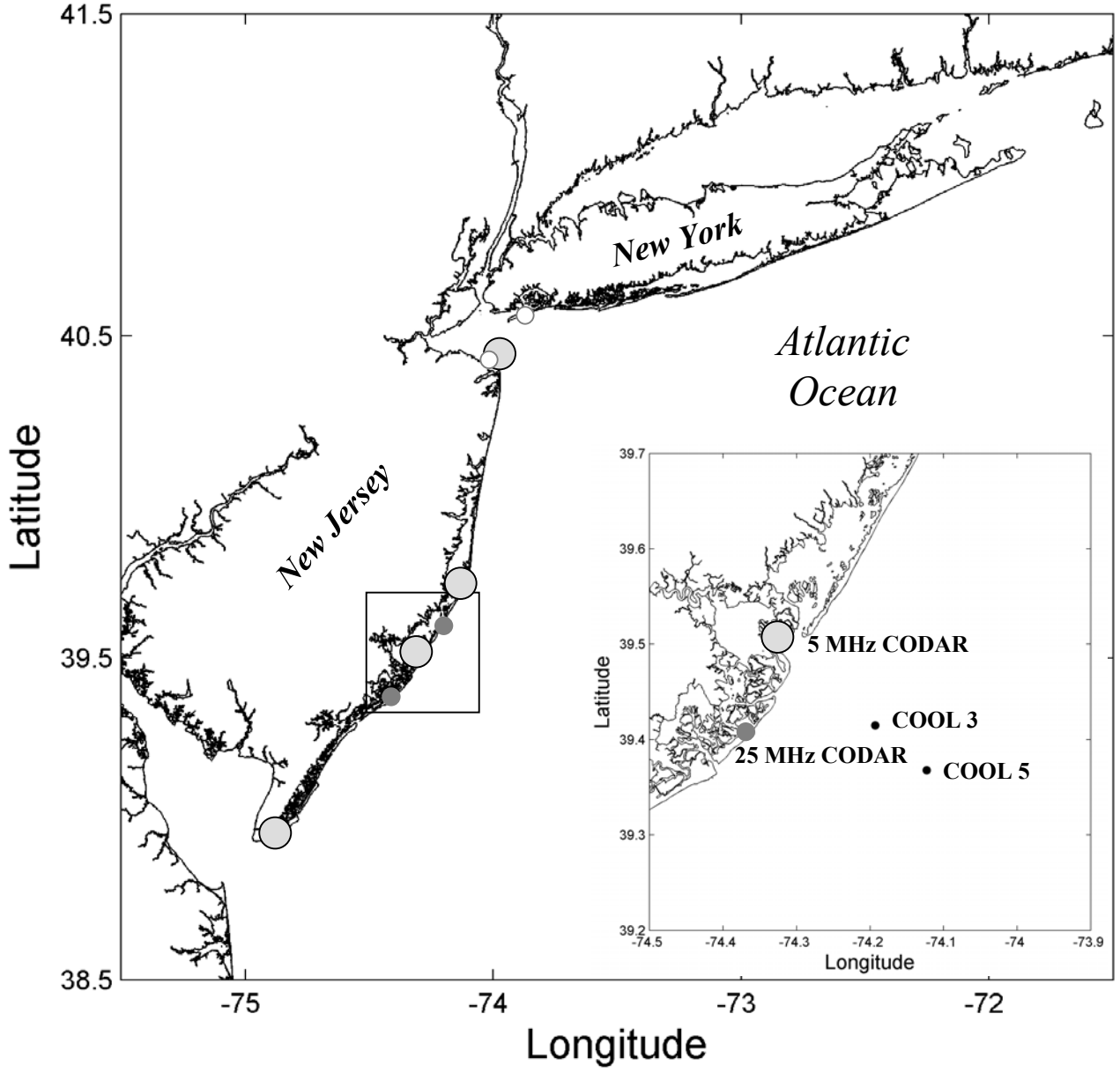

Figure 1: Study site off the coast of New Jersey. The location of the long-range (light gray), original standard range (dark-gray), and present standard-range (white) are shown. The inset shows the locations of the ADCPs and the two CODAR sites discussed here.

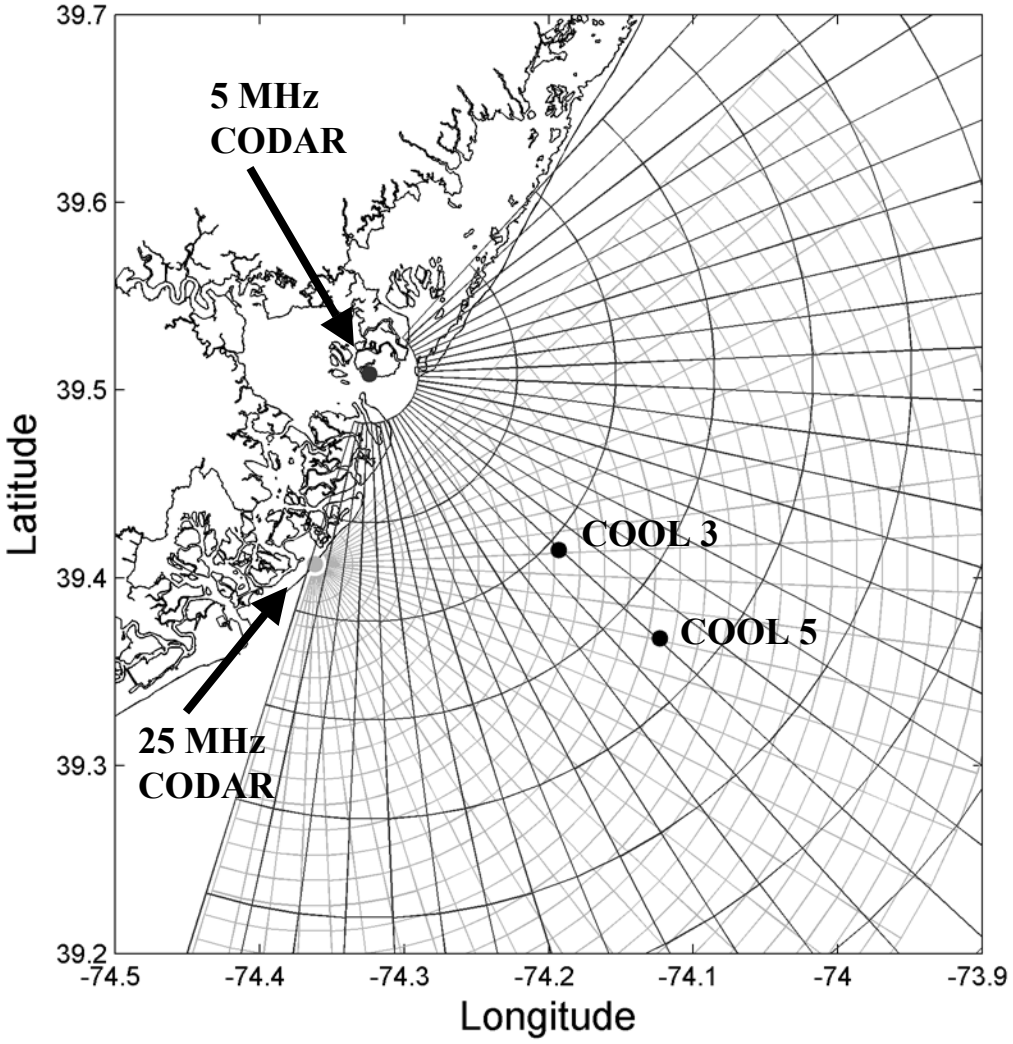

Figure 2: The radial data girds for the 5MHz system (dark gray) and the 25 MHz system (light gray). The locations of the ADCPs are also shown.

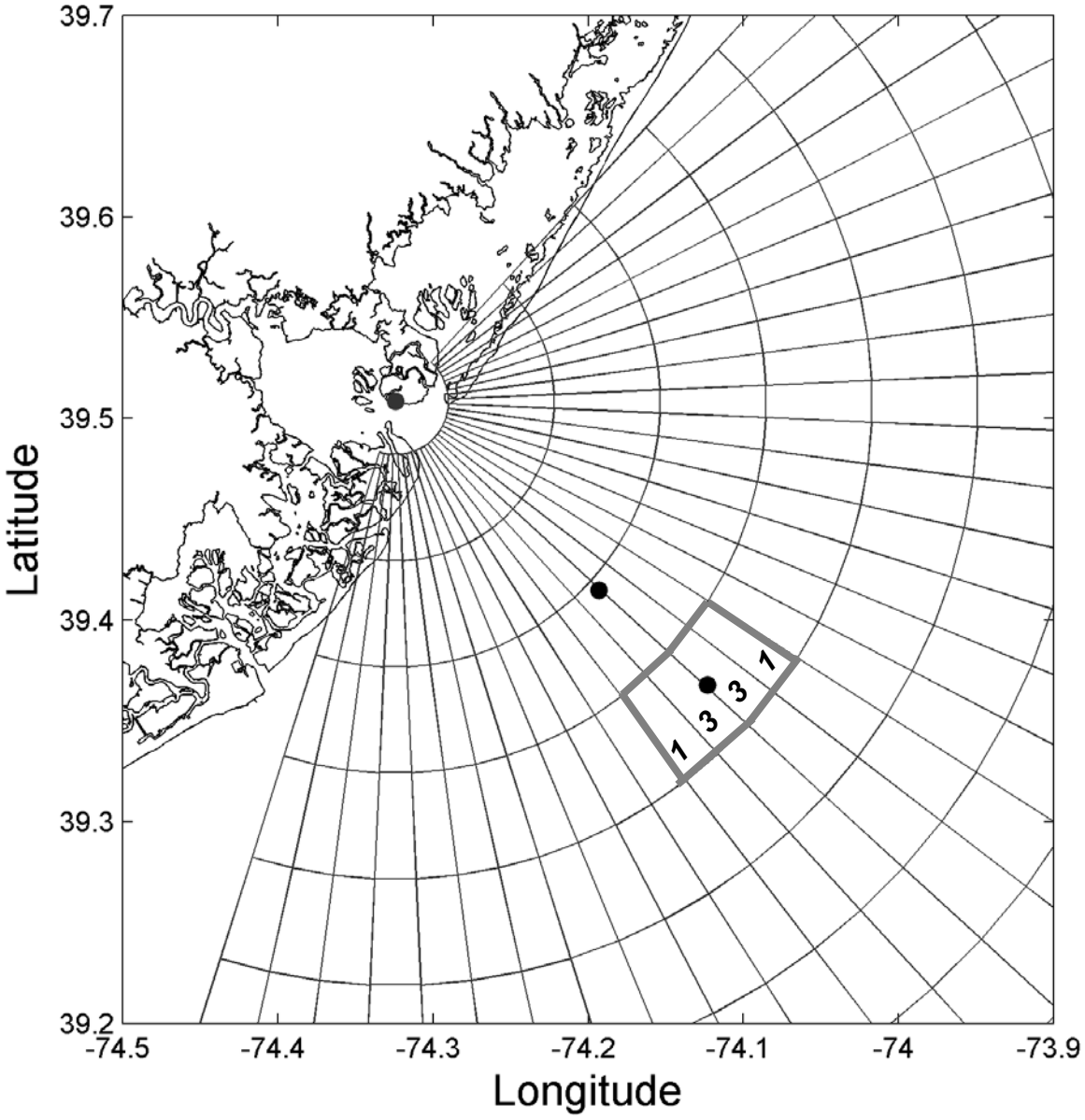

Figure 3: The four cells used in the interpolation. Their relative weights are indicated within each cell.

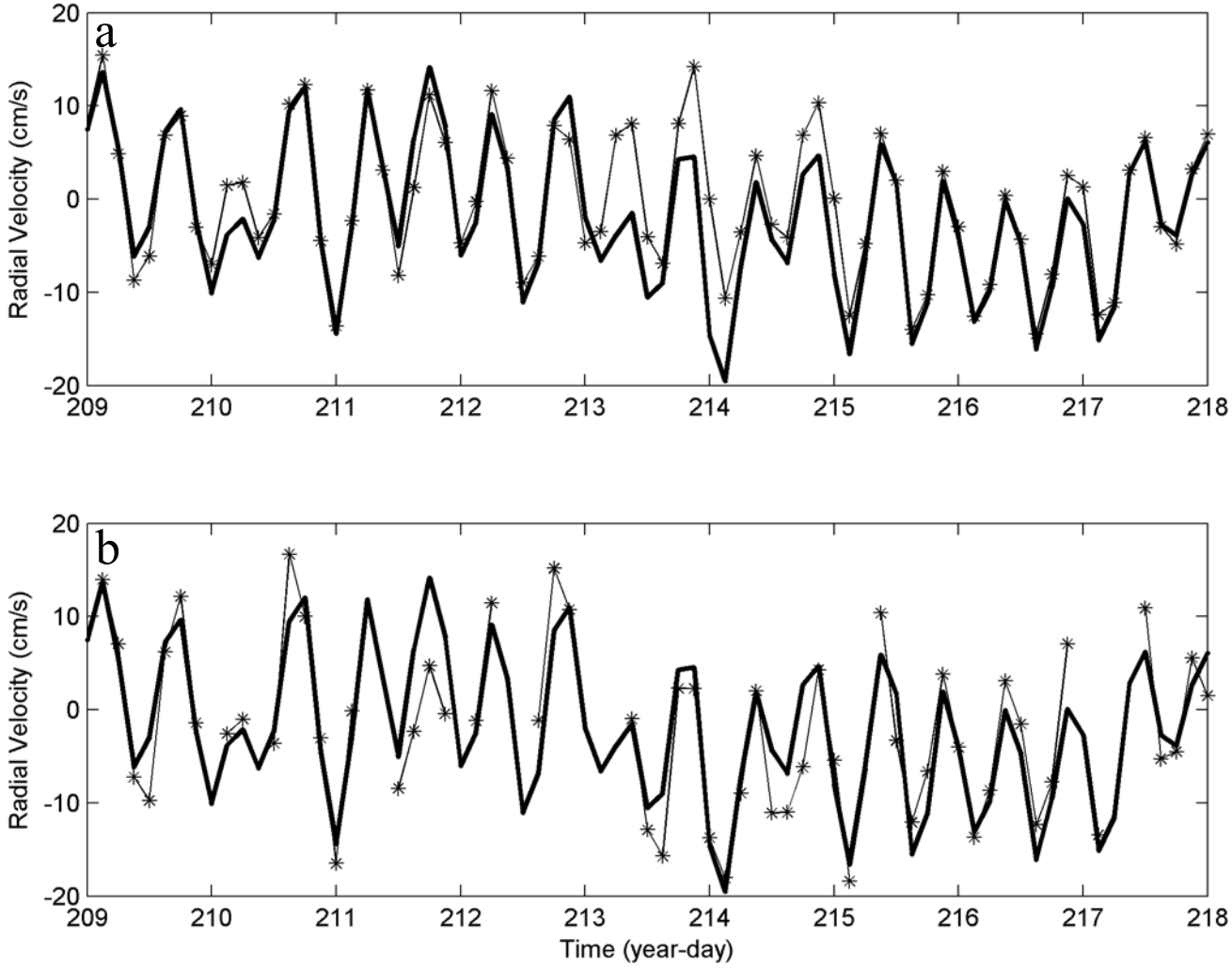

Figure 4. (a) Time series of the cross-shore velocity of the ADCP5 bin at 3.5 m depth (thick) and the ADCP5 bin at 6.5 m depth (thin). (b) Time series of the cross-shore velocity of the ADCP5 bin at 3.5 m depth (thick) and CODAR at the surface (thin).

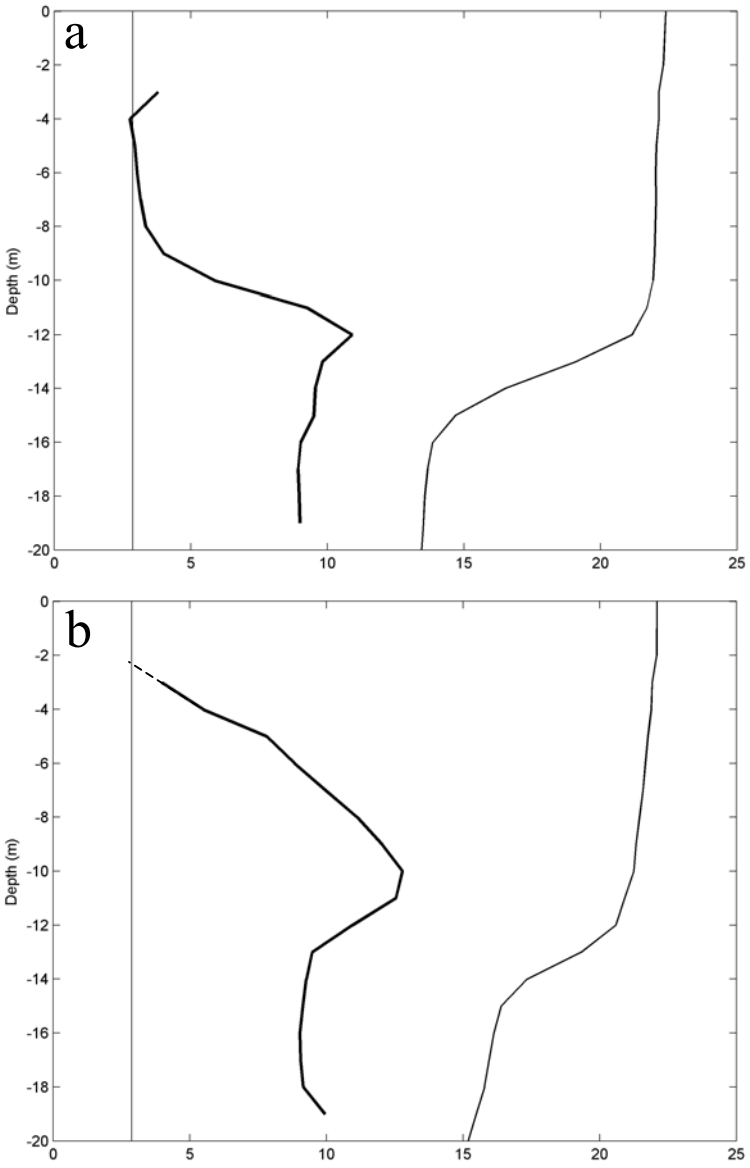

Figure 5. The depth profile of the mean temperature [°C] (thin) and RMS difference [cm/s] between the CODAR surface measurement and each bin of the ADCP at COOL5 (thick) for a (a) low shear time [yd 209-210] and a (b) high shear time [213-214]. The thin black lines at 2.82 (a) and 2.88 (b) are the rms difference between the surface bin at COOL5 and the surface bin at COOL3 over the respective time period. The extrapolated RMS difference is shown as a dashed line.

	Frequency (MHz)	Sweep Rate (Hz)	FFT Length (minutes)	Spectra Average (minutes)	Currents Average (hours)	Output Frequency (hours)	Depth of Measurement (m)	Spatial Coverage of Measurement (km^2)
ADCP	0.60	0.5	NA	NA	Match CODAR	Match CODAR	3.5 (top bin)	0.00012
Long-range CODAR	4.55	1.0	17.07	60	4	3	1.6	12
Standard range CODAR	24.70	2.0	4.27	15	1.25	1	0.3	3

Table I. Operating settings for the ADCPs, Long-range, and Standard-range CODAR systems.

# pts	Cool 5 Bin 17 (cm/s)	Cool 3 Bin 15 (cm/s)
1	4.27	3.63
2	2.82	2.25
3	1.86	1.78
4	1.47	1.22
5	1.04	0.92
6	0.70	0.59
7	0.00	0.00

Table II. RMS difference between ADCP time series with varying number of points going into each four-hour average and the complete record with all seven points going into each four hour average.

			Raw Velocity (cm/s)	Tidal Velocity (cm/s)
COOL5 ADCP (3.5m)	vs	COOL5 ADCP (6.5m)	**6.25**	**0.63**
COOL5 ADCP (3.5m)	vs	COOL3 ADCP (3.5m)	**5.22**	**1.22**
CODAR	vs	COOL5 ADCP (3.5m)	**5.86**	**0.71**
CODAR	vs	COOL3 ADCP (3.5m)	**6.30**	**2.22**
CODAR (Interpolated)	vs	COOL5 ADCP (3.5m)	**4.98**	**0.18**
CODAR (Standard Range)	vs	COOL5 ADCP (3.5m)	**6.40**	**0.97**

Table III. RMS difference statistics.